Corrosion of Selected Hard Facing Materials Exposed to Mine Water

S.I. Hango[1,2,3,4]*, L.H. Chown[1,2,3], J.W. van der Merwe[1,2,3]
F.P.L. Kavishe[1,4], L.A. Cornish[1,2,3]

[1]African Materials Science and Engineering Network (AMSEN - A Carnegie-IAS Network).

[2]School of Chemical and Metallurgical Engineering, University of the Witwatersrand, South Africa.

[3]DST-NRF Centre of Excellence in Strong Materials, University of the Witwatersrand, South Africa.

[4]Faculty of Engineering and Information Technology, University of Namibia, Namibia

Abstract

Corrosion damage can cause major failure of mining pumps which could lead to degradation of other mining equipment, as a result of leakage, thus leading to a high rate of replacement and maintenance of pumps and surrounding equipment. Hard facing materials are used to protect moving parts against mechanical and corrosion damage. The corrosion behavior of a corrosion resistant Hastelloy G30 and a hard facing material, a nickel-chromium-iron (Ni-Cr-Fe) alloy (both high chromium nickel-based alloys) exposed to synthetic and acidified mine water were studied using potentiodynamic polarisation. The results showed lower corrosion rates for Hastelloy G30 than for Ni-Cr-Fe. The corrosion rates at pH 6.8, at ambient temperature and 35°C were 0.00011 mm.y^{-1} and 0.00035 mm.y^{-1} for Hastelloy G30; 0.0016 mm.y^{-1} and 0.0017 mm.y^{-1} for INCONEL Alloy 600, and at pH 3, at ambient temperature and 35°C corrosion rates were 0.0003 mm.y^{-1} and 0.00083 mm.y^{-1} for Hastelloy G30; 0.1 mm.y^{-1} and 3.2 mm.y^{-1} for INCONEL Alloy 600. The microstructures of the alloys before and after corrosion tests were characterised using optical microscopy; X-ray diffraction (XRD), and microhardness measurements were also performed.

Keywords: corrosion, synthetic mine water, hard facing.

ISTJN 2014; 4:90-105.

*Corresponding author -E-mail address: shango@unam.na.

1 Introduction

Corrosion is a common cause of failure in mining and mineral processing industries, leading to failures of various components, such as pumps, valves, couplings, etc. in acidic and alkaline environments (Yoganandh et al. 2013). The results of corrosion effects usually lead to leakage, high rate of replacement and maintenance. In underground mines, there are SO_4^{2-}, Na^+, Ca^+, Mg^{2+} and Cl^- in the water with different pH values, and CH_4, CO, CO_2, as well as H_2S and SO_2 in the air. These create an erosive-corrosive environment (Lalvani et al. 1990; Wang et al. 1997; White and Higginson 1985). Carter (1986), Al-Bukhaiti et al. (2007) and Llewellyn et al. (2004) studied factors that affect the corrosion in mining industry and processing plants, such as material properties and pH. They found that steels with less carbon and chromium contents experienced erosive-corrosive and abrasive wear, resulting in ploughing, microcutting, indentation with lips as well as fracture and cracking of carbide phases and fatigue wear.

Hard facing materials protect metal equipment from wear or abrasion (Clark 1985), and are applied as a surface layer on an underlying material, usually low or medium carbon steels (Rodríguez 2003), by depositing a special alloy (the 'hard face') on the substrate, using various welding processes, to improve wear properties and/or dimensions (Berns and Fischer 1986). Hastelloy G30 and INCONEL Alloy 600 hard facing materials are both high-chromium nickel-based alloys, which form a thin passive film when the alloys are immersed in a liquid environment, giving low corrosion rates (Jena and Chaturvedi 1984; Zhang et al. 2012). This makes them useful for improved corrosion resistance in underground mine equipment, especially water pumps and pipes carrying aggressive mine waters. Hastelloy G30 (also known as UNS N06030) is a nickel-based alloy suitable for handling phosphoric, sulphuric and nitric acids, while INCONEL Alloy 600 (also known as UNS N06600) is also a nickel-based alloy with various uses, especially in pump systems operating in highly corrosive environments (HAYNES 2013). This alloy may be hard faced on low or medium carbon steels to protect against mechanical and chemical attack (Rodríguez 2003). The chemical compositions of the two high-chromium nickel-based alloys are given in Table 1 (HAYNES 2013).

This study includes potentiostatic polarisation measurements in synthetic mine water (a simplified underground mining industrial solution), and optical microscopy, X-ray diffraction (XRD) and microhardness measurements.

Table 1: Typical chemical compositions of the test materials (wt%) (HAYNES 2013).

Composition	Sample	
	Hastelloy G30	INCONEL Alloy 600
Ni	Balance	Balance
Co	5.00	0.30
Cr	28.00–31.50	16.60
Mo	4.00–6.00	0.04
W	1.50–4.00	-
Fe	13.00–17.00	4.03
Si	0.80	4.49
Mn	1.50	0.20
Al	-	0.02
C	0.03	0.06
Nb+Ta	0.30–1.50	-
Cu	1.00–2.40	-
P	0.04	-
S	0.02	-
Nb	-	0.01

2   Experimental Procedure

The Hastelloy G30 and INCONEL Alloy 600 samples were cut, hot mounted in epoxy resin, ground to 1200 grit, and polished to 1 μm for optical microscopy, hardness measurements and XRD analyses. The Hastelloy specimen was etched electrolytically in 5 g oxalic acid and 95 ml HCl, at 6 V DC for 5 seconds. INCONEL Alloy 600 was etched in equal parts of HCl, HNO_3 and acetic acid, swabbing for 1 minute at room temperature.

The microstructures were examined before and after the corrosion measurements in a Leica CTR6000 optical microscope. Hardness measurements were performed using an FM-700 Vickers Microhardness tester, with a 2 kg load (HV_2), and five measurements were made with the average being reported.

Samples were prepared metallographically for X-ray diffraction analyses before and after corrosion experiments. A BRUKER D2 PHASER diffractometer was used, with Cobalt 2θ radiation at 30 kV and 10 mA. Diffractograms were recorded in a non-spinning regime, at an angle $2\theta = 20°$ to $140°$.

The samples were cold-mounted in epoxy resin, ground to 1200 grit for corrosion measurements, and the exposed areas of the samples to the corrosive environment were measured.

The measurements were carried out in synthetic mine water (pH=6.8) of the composition given in Table 2, at ambient temperature (22°C) and at 35°C in a water bath. The synthetic mine water was prepared from a mixture of salts: magnesium and sodium sulphates, calcium and sodium chlorides into de-ionised water, and acidified with 32% HCl to a pH 3. It was measured for conductivity (using an ORION STAR A212 conductivity meter), total dissolved solids (TDS), salinity, resistivity, pH (using an ORION STAR A211 pH meter), cations (Na^+, Ca^{2+} and Mg^{2+}) and anions (SO_4^{2-} and Cl^-) using atomic absorption spectroscopy (AAS), inductively coupled plasma optical emission spectroscopy (ICP-OES) at Mintek, Randburg, South Africa.

Table 2: Composition of synthetic mine water solution used in the measurements (Wang et al. 1997; White and Higginson 1985).

Salt	Concentration (mg.L^{-1})
MgSO$_4$	198
Na$_2$SO$_4$	1215
CaCl$_2$	1038
NaCl	1379

Potentiodynamic polarization measurements were performed using an Auto Tafel Potentiostat V1.79 and Auto LPR V2.7h software at a scan rate of 0.166 mV.s^{-1} after a 30 minute open circuit scan, to stabilise the potential applied, and their electrochemical responses were studied. The corrosion current density (i_{corr}) of the samples was obtained from the measured linear polarization resistance (LPR) using the Stern-Geary equation (Kelly et al. 2002):

$$i_{corr} = \frac{1}{2.3R_p}\left(\frac{\beta_a\beta_c}{\beta_a+\beta_c}\right) = \frac{B}{R_p} \tag{1}$$

where β_a = anodic Tafel slope, β_c = cathodic Tafel slope ($\beta_a = \beta_c = 0.1$), R_p = polarization resistance and, B = proportionality constant. The corrosion rates in mm.y^{-1} were calculated by using Equation 2:

$$\text{Corrosion rate}(CR) = \left(\frac{0.00327E_w}{\rho}\right)i_{corr} \tag{2}$$

where E$_w$ = equivalent weight of alloy (g), ρ = the density of alloy (g.cm^{-3}) and i_{corr} = corrosion current density (μA.cm^{-2}).
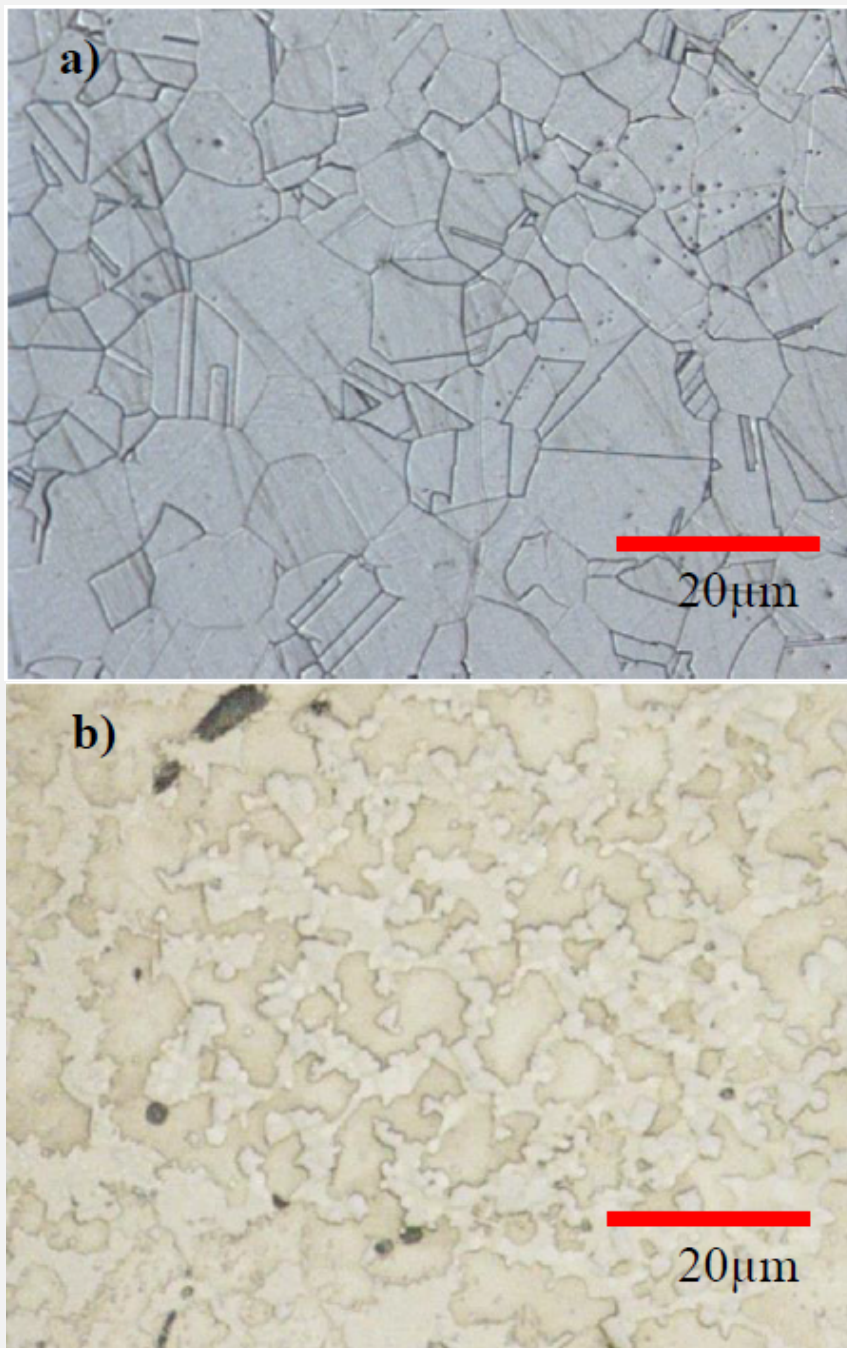
Figure 1: Optical micrographs of: a) Hastelloy G30, showing equiaxed and twinned γ; and b) INCONEL Alloy 600, showing Ni-Cr (light) and Cr- and Mo-carbides (dark).
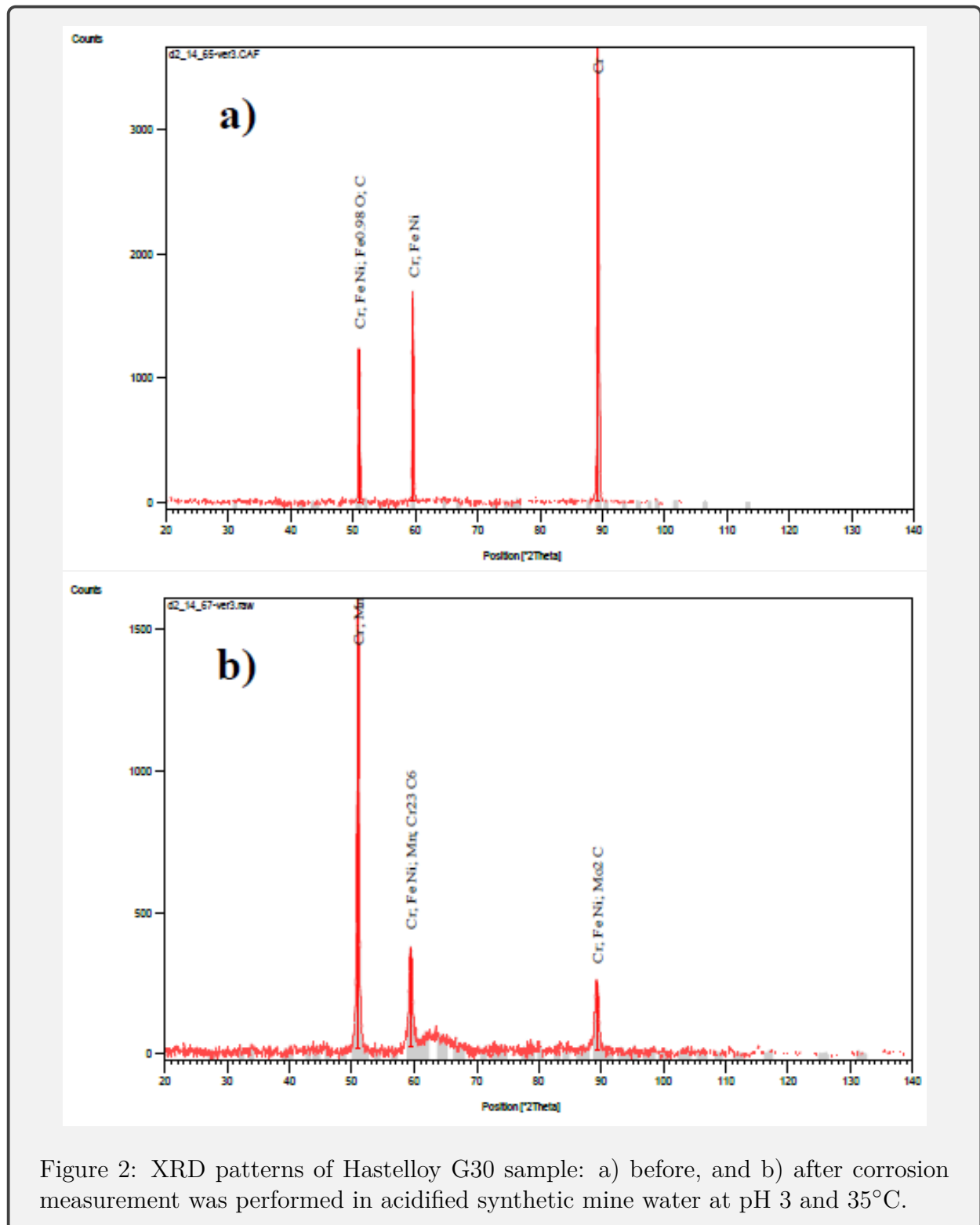
Figure 2: XRD patterns of Hastelloy G30 sample: a) before, and b) after corrosion measurement was performed in acidified synthetic mine water at pH 3 and 35°C.
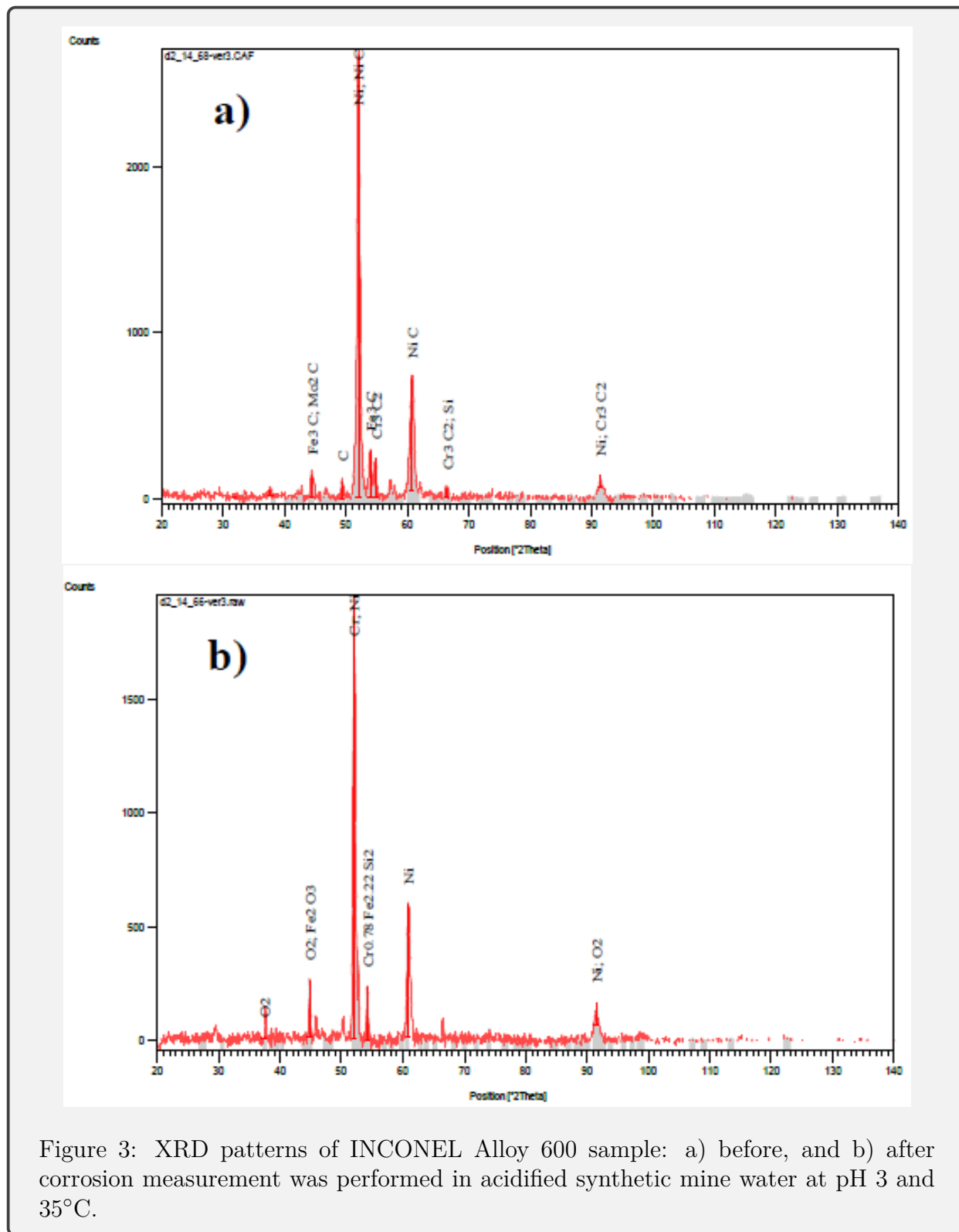
Figure 3: XRD patterns of INCONEL Alloy 600 sample: a) before, and b) after corrosion measurement was performed in acidified synthetic mine water at pH 3 and 35°C.

3 Results

3.1 Microstructural and Hardness Characterisation

Optical micrographs of the Hastelloy G30 and INCONEL Alloy 600 before testing are shown in Figure 1. Hastelloy G30 had well defined grain boundaries with equiaxed grains and mechanical twins, while INCONEL Alloy 600 had a two-phase structure, and irregular grain boundaries of Ni-Cr and carbide phases. These were confirmed by XRD analyses. INCONEL Alloy 600 had a hardness of $652\pm36HV_2$, and the Hastelloy G30 hardness was $176\pm6HV_2$.

3.2 XRD Analyses

X-ray diffraction was performed before and after the corrosion measurements in synthetic mine water and are shown in Figures 2-3. The Hastelloy G30 had Ni, Cr, Mn, FeNi, Mo_2C, $Cr_{23}C6$ and C before the corrosion tests, and only Cr, Fe, FeNi, NiO, $Fe_{0.98}O$ and C on the surface after corrosion. For INCONEL Alloy 600, the same species as in Hastelloy G30 were detected before corrosion, as well as Si. After corrosion, Cr, Ni, O_2, Fe_2O_3 and $Cr_{0.78}Fe_{2.22}Si_2$ were present.

Table 3: Electrochemical test results of Hastelloy G30 and INCONEL Alloy 600 alloy in synthetic mine water.

Sample	pH	Temperature (°C)	E_{corr} (mV)	i_{corr} ($\mu A.cm^{-2}$)	Corrosion rate ($mm.y^{-1}$)
Hastelloy G30		Ambient	-200	0.011	0.00011
INCONEL Alloy 600	6.8		-267	0.17	0.0016
Hastelloy G30		35	-153	0.035	0.00035
INCONEL Alloy 600			-319	0.17	0.0017

3.3 Electochemical Measurements

Figure 4 shows the corrosion products on the surface of the samples. Hastelloy G30 had a surface film with cracks, and with some corrosion products, while INCONEL Alloy 600 had microcracks in the corrosion products. Figures 5 and 6 show the polarisation curves for both alloys in synthetic and acidified mine water. The corrosion potential (E_{corr}) of Hastelloy G30 was higher than that of INCONEL Alloy 600, and a higher corrosion rate
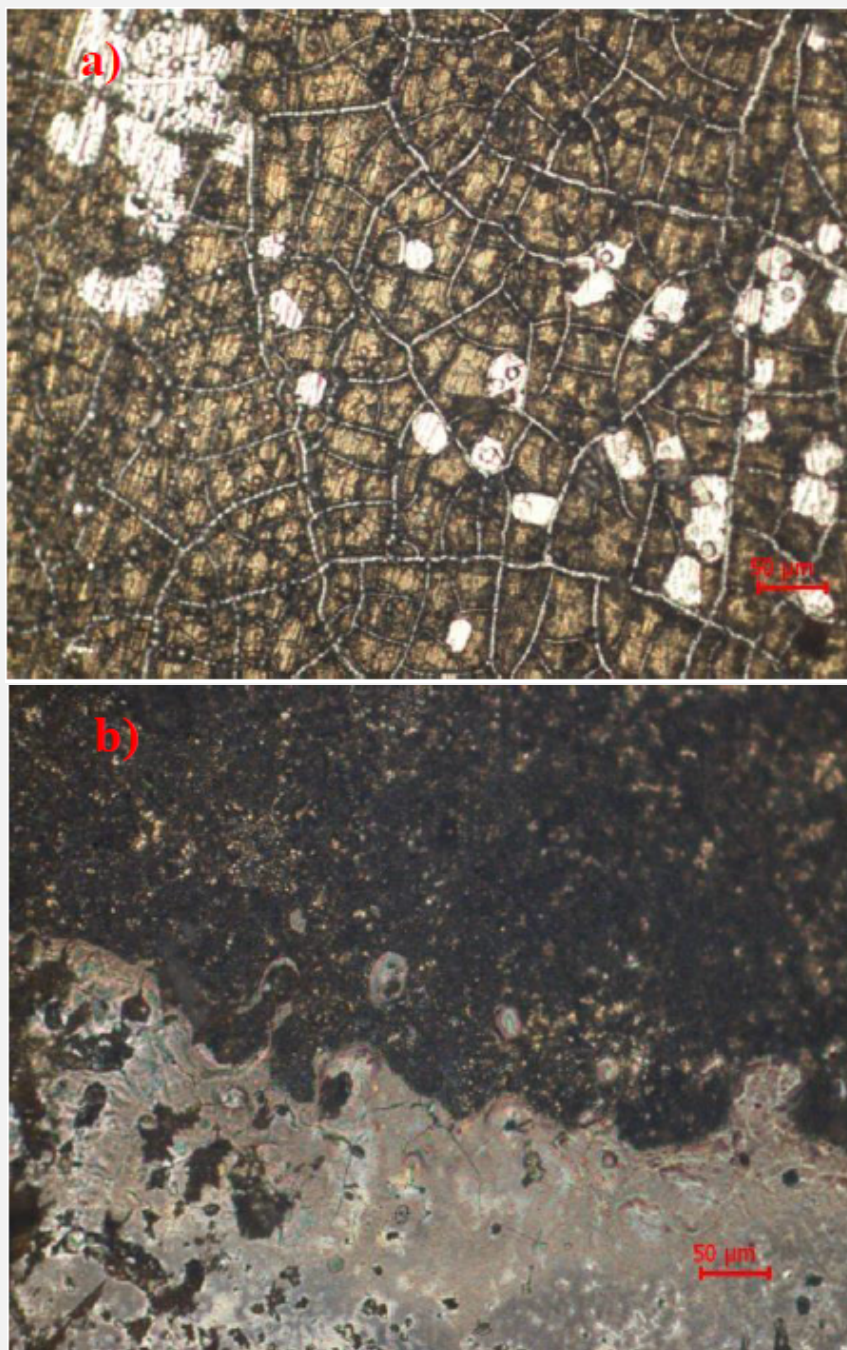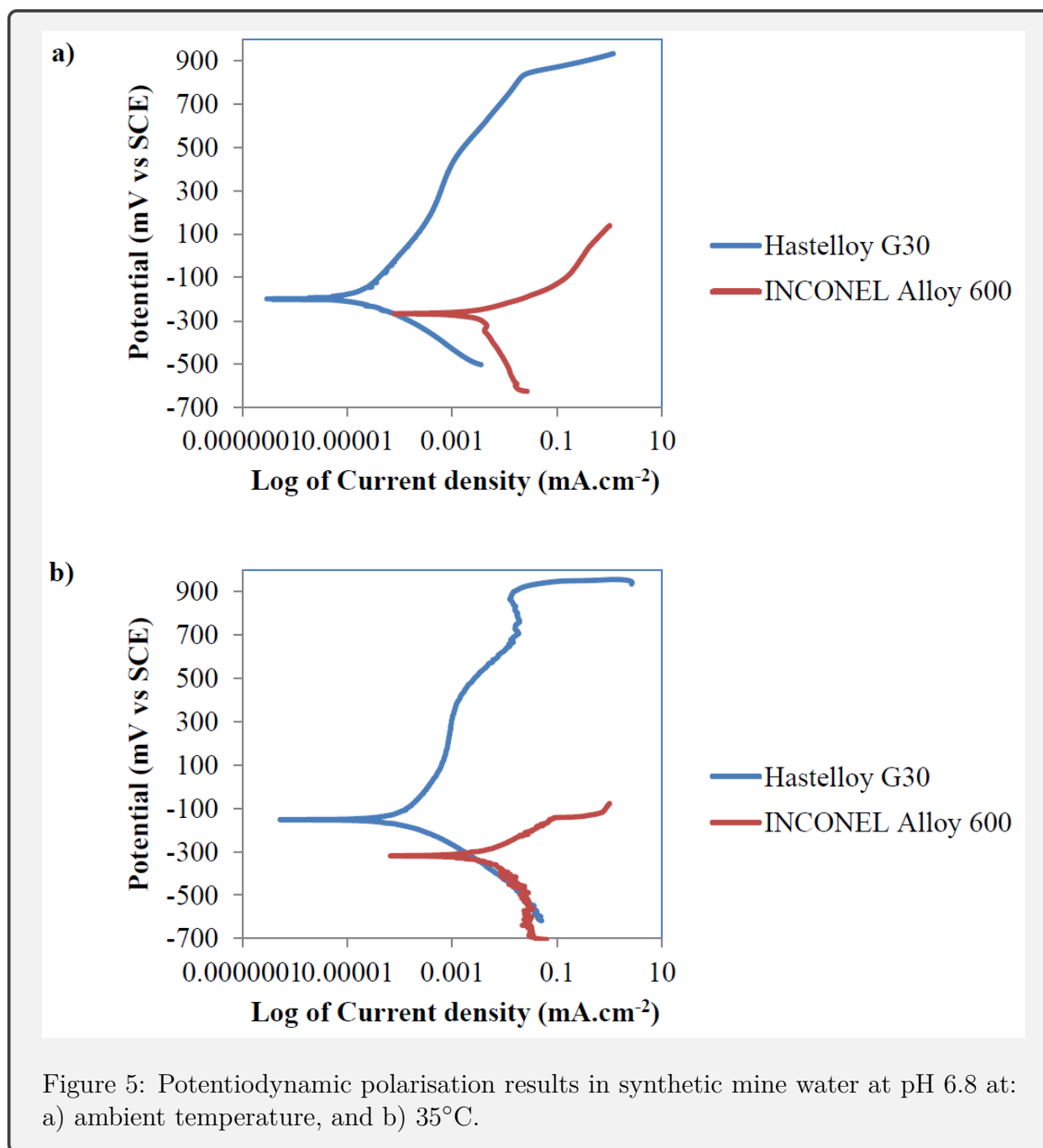
Figure 4: Optical micrographs taken after corrosion measurements in synthetic mine water at pH 3 and 35°C, for: a) Hastelloy G30, showing cracks in the protective film and some white corrosion products; and b) INCONEL Alloy 600, showing microcracks in the corrosion products.
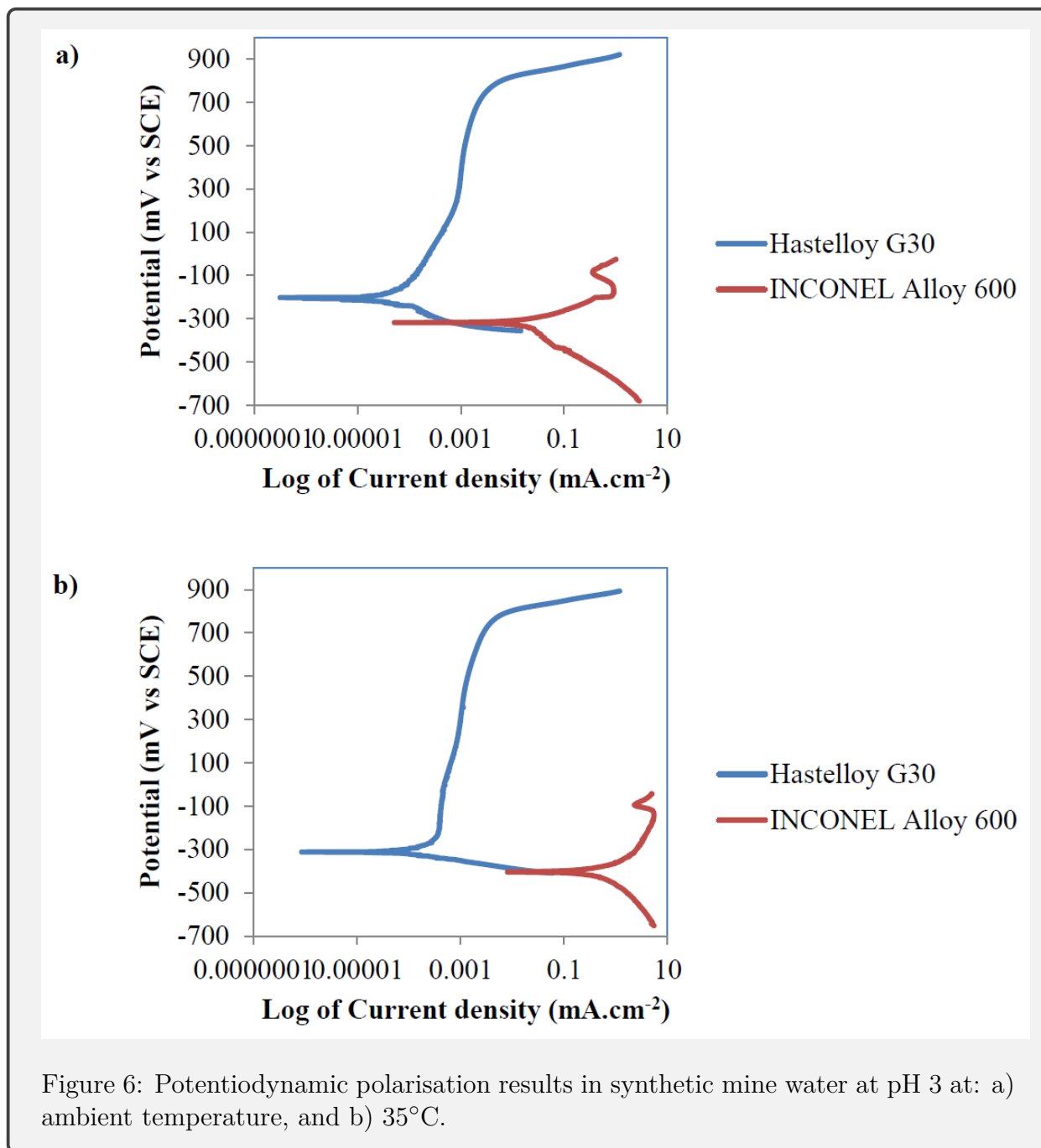
Figure 5: Potentiodynamic polarisation results in synthetic mine water at pH 6.8 at: a) ambient temperature, and b) 35°C.

Figure 6: Potentiodynamic polarisation results in synthetic mine water at pH 3 at: a) ambient temperature, and b) 35°C.

Table 4: Electrochemical test results of Hastelloy G30 and INCONEL Alloy 600 in acidified synthetic mine water.

Sample	pH	Temperature ($°$C)	E_{corr} (mV)	i_{corr} (μA.cm^{-2})	Corrosion rate (mm.y^{-1})
Hastelloy G30		Ambient	-207	0.033	0.0003
INCONEL Alloy 600	3		-318	1.1	0.1
Hastelloy G30		35	-312	0.091	0.00083
INCONEL Alloy 600			-405	3.3	3.2

was observed on INCONEL Alloy 600. Hastelloy G30 experienced a slight spontaneous passivation and high breakaway potentials in the solutions tested, with more evidence of pitting in synthetic mine water at 35°C. INCONEL Alloy 600 had no passivation behaviour in all other solutions tested other than in synthetic mine water at pH 3 at 35°C. From these observations, it can be concluded that alloys were more resistant to synthetic mine water than to acidified synthetic mine water. The summary of the electrochemical results is given in Tables 3-4. Table 5 shows properties of synthetic and acidified synthetic mine water.

4   Discussion

Optical microscopy showed that Hastelloy G30 had equiaxed and twinned γ, while INCONEL Alloy 600 had Ni-Cr and Cr-Mo-carbide phases, which were confirmed by XRD analyses. The micrographs also showed that the surface layers (consisting of corrosion products) of the INCONEL Alloy 600 were more severely damaged than the Hastelloy G30. This behavior is caused by the presence of SO_4^{2-} and Cl^- in solution (Li et al. 2001). From the microstructures, it can be concluded that the lower surface damage of the Hastelloy G30 than INCONEL Alloy 600 in all conditions tested was probably due to the higher chromium content in Hastelloy G30, making the surface more resistant to damage by ions in the solutions by forming a more protective film on the surface of Hastelloy G30 (Hayes et al. 2006). Additionally, lower corrosion damage of Hastelloy G30 was also due to its higher Mo and W contents which stabilize the protective film on the surface. The surface layers were probably uniform, and they cracked during drying (Jakupi et al. 2011) when the air reacted with the film formed on the surface of the sample after corrosion measurements in saline environments. XRD patterns showed Fe_2O_3, NiO and $Fe_{0.98}O$ which were corrosion products for both alloys.

Tables 4 and 5 show that the potentiodynamic polarization responses of Hastelloy G30 in synthetic and acidified synthetic mine water at pH 6.8 and 3 had a lower corrosion current

Table 5: Properties of synthetic and acidified synthetic mine water for corrosion measurements.

Properties	Synthetic mine water	Acidified synthetic mine water
Conductivity (μS.cm^{-1})	4.9	12.9
TDS (ppt)	2.7	6.4
Salinity (psu)	2.9	7.5
Resistivity (Ohm.cm)	183.5	76.9
pH	6.8	3
SO_4^- (ppm)	1007	1043
Na^+ (ppm)	928	890
Ca^{2+} (ppm)	108	111.5
Cl^- (ppm)	1700	2600
Mg^{2+} (ppm)	11	12

density (i_{corr}) than INCONEL Alloy 600 in all solutions and conditions measured, and hence Hastelloy G30 had a lower corrosion rate than INCONEL Alloy 600. Hastelloy G30 experienced a slight spontaneous passivation and high breakaway potentials in the solutions tested, with more evidence of pitting in synthetic mine water at 35°C. INCONEL Alloy 600 had no passivation behaviour in all other solutions tested, other than in synthetic mine water at pH 3 at 35°C. However, INCONEL Alloy 600 experienced repassivation behaviour after breakaway potential in all conditions tested due to the presence of molybdenum content in the alloy (Hayes et al. 2006).

INCONEL Alloy 600 (652±36HV$_2$) was much harder than Hastelloy G30 (176±6HV$_2$) because of Cr^- and Mo^- carbides, which formed in the presence of Si (Pigrova et al. 1980). The hardness values of the samples are important for exposure to erosion-corrosion conditions due to particles in mine water that would cause wear (Wood 2007). The hard face surface can be heat treated without affecting the substrate by laser heat treatment. Bolelli et al. (2008) worked on laser heat treatment of cobalt and nickel alloys, which resulted in iňĄne-grained carbides (improving hardness), and more noble values of corrosion potential and decreased corrosion current density (improving corrosion resistance) by improving inter-lamellar cohesion. INCONEL Alloy 600 is therefore recommended as a hard facing material in mine water conditions, and may be treated similarly to improve its resistance to corrosion and wear.

When the pH of the solution was decreased, the values of conductivity, total dissolved solids (TDS) and salinity increased with a decrease in resistivity. Thus, the acidified synthetic mine water should be more corrosive than synthetic mine water.

The results showed that acidified synthetic mine water had more suspended particles, high conductivity, salinity, and low resistivity and pH as well as high concentration of SO_4^{2-},

Ca^{2+}, Cl^- and Mg^{2+} than the synthetic mine water, making it to be the most aggressive environment.

5 Conclusions

- INCONEL Alloy 600 ($652\pm36HV_2$) was much harder than Hastelloy G30 ($176\pm6HV_2$), making it more suitable to operate effectively in abrasive wear conditions.

- Potentiodynamic polarization responses of Hastelloy G30 sample in synthetic and acidified synthetic mine water at pH 6.8 and 3 showed a lower corrosion current density (i_{corr}) than INCONEL Alloy 600 in all solutions and conditions measured. Hastelloy G30 is more a corrosion resistant material in synthetic mine water than INCONEL Alloy 600.

- When the pH of the solution was decreased, the values of conductivity, total dissolved solids (TDS) and salinity increased with decreased resistivity, hence the acidified synthetic mine water was more corrosive than synthetic mine water.

- INCONEL Alloy 600 is recommended as a hard facing material in mine water conditions.

References

[1] Al-Bukhaiti MA, Ahmed SM, Badran FMF, Emara KM. Effect of impingement angle on slurry erosion behaviour and mechanisms of 1017 steel and high-chromium white cast iron. Wear 262, 1187-1198 (2007).

[2] Berns H, Fischer A. Abrasive wear resistance and microstructure of Fe-Cr-C-B hard surfacing weld deposits. Wear 112, 163-180 (1986).

[3] Bolelli G, Lusvarghi L, Barletta M. Heat treatment effects on the corrosion resistance of some HVOF-sprayed metal alloy coatings. Surf. and Coat. Tech. 202, 4839-4847 (2008).

[4] Carter AMF. Erosion, corrosion, and abrasion of material handling systems in the mining industry. J. S. Afr. Inst. Min. Metall. 86, 235-242 (1986).

[5] Clark WP. 'High Tech' hardfacing alloys combat corrosion and abrasion of metal parts. Welding J. 64, 69-71 (1985).

[6] Hayes JR, Gray JJ, Szmodis AW, Orme CA. Influence of chromium and molybdenum on the corrosion of nickel-based alloys. Corrosion 62, 491-500 (2006).

[7] HAYNES International. Corrosion-resistant alloys. HAYNES International Website. `http://www.haynesintl.com/cralloys.htm`. Accessed April 2013.

[8] Jakupi P, Wang F, Noël JJ, Shoesmith DW. Corrosion product analysis on crevice corroded Alloy-22 specimens. Corr. Sci. 53, 1670-1679 (2011).

[9] Jena AK, Chaturvedi MC. The role of alloying elements in the design of nickel-base superalloys. J. Mat. Sci. 19, 3121-3139 (1984).

[10] Kelly RG, Scully JR, Shoesmith D, Buchheit RG. Electrochemical Techniques in Corrosion Science and Engineering. Marcel Dekker, Inc. New York, USA (2002).

[11] Lalvani SB, Swisher JH, Pagano MA. A review of chlorine-induced corrosion in underground mines and coal preparation plants. Fuel Pr. Tech. 25, 17-32 (1990).

[12] Li L, Sagues A. Metallurgical effects on Chloride ion corrosion threshold of Steel in cocnrete. Technical report to Department of Transportation. University of South Florida. No. WPI 0510806 (2001).

[13] Llewellyn RJ, Yick SK, Dolman KF. Scouring erosion resistance of metallic materials used in slurry pump service. Wear 256, 592-599 (2004).

[14] Pigrova GD, Korkka SI, Grebtsova TM. Effect of silicon on the phase composition of nickel-base alloys. Met. Sci. and Heat Treat. 22, 274-277 (1980).

[15] Rodríguez J, Guerrero-Mata M, Colás R. Crack propagation in a hard-faced AISI type 304 stainless steel. Mat. Char. 51, 95-99 (2003).

[16] Wang P-Z, Yang Y-S, Ding G, Qu J-X, Shao H-S. Laser cladding coating against erosion-corrosion wear and its application to mining machine parts. Wear 209, 96-100 (1997).

[17] White RA, Higginson A. Factors affecting the corrosivity of underground minewater. Proc. Mintek 50, Int. Conf. on Min. Sci. and Tech. Sandton, South Africa. 26-30 March 1984 (1985).

[18] Wood RJK. Tribo-corrosion of coatings: a review. J. Phys. 40, 5502-5521 (2007).

[19] Yoganandh J, Natarajan S, Kumaresh Babu SP. Erosive wear behavior of nickel-based high alloy white cast iron under mining conditions using Orthogonal Array. J. Mat. Eng. and Perf. 22, 2534-2541 (2013).

[20] Zhang D-K, Wang S-Q, Shen Y, Ge S-R. Interactive mechanisms of fretting wear and corrosion of steel wires in alkaline corrosion medium. Proc. Inst. Mech. Eng. J. Eng. Tribology 226, 738-747 (2012).